Spin Hall effect due to intersubband-induced spin-orbit interaction in symmetric quantum wells

Minchul Lee,[1] Marco O. Hachiya,[2] E. Bernardes,[2] J. Carlos Egues,[2,3] and Daniel Loss[3]

[1]*Department of Applied Physics, Kyung Hee University, Yongin 449-701, Korea*
[2]*Instituto de Física de São Carlos, Universidade de São Paulo, 13560-970 São Carlos, SP, Brazil*
[3]*Department of Physics, University of Basel, CH-4056 Basel, Switzerland*

We investigate the intrinsic spin Hall effect in two-dimensional electron gases in quantum wells with two subbands, where a new intersubband-induced spin-orbit coupling is operative. The bulk spin Hall conductivity σ_{xy}^z is calculated in the ballistic limit within the standard Kubo formalism in the presence of a magnetic field B and is found to remain finite in the $B=0$ limit, as long as only the lowest subband is occupied. Our calculated σ_{xy}^z exhibits a nonmonotonic behavior and can change its sign as the Fermi energy (the carrier areal density n_{2D}) is varied between the subband edges. We determine the magnitude of σ_{xy}^z for realistic InSb quantum wells by performing a self-consistent calculation of the intersubband-induced spin-orbit coupling.

I. INTRODUCTION

The spin Hall effect (SHE) (Ref. 1) refers to the spin accumulation with opposite polarizations at the two edges of a Hall bar due to the transverse spin current induced by a driving longitudinal charge current. This effect was first theoretically proposed[2] as arising from the spin-dependent scattering at impurities with spin-orbit (SO) interaction. In the literature this is commonly referred to as the "extrinsic SHE" as it relies on the presence of impurities ("extrinsic mechanism"). In this case, the asymmetric Mott-skew and side-jump scattering contributions drive spin-up and spin-down electrons toward opposite directions, thus giving rise to a net transverse spin current (with no charge current) and to spin accumulation at the edges. Recently, two theoretical works[3,4] predicted that the spin-orbit effects on the band structure of semiconductors—the so called "intrinsic mechanism" for the SHE—can also give rise to a spin current perpendicular to an applied electric field, even in the absence of impurities. These authors have calculated the ballistic spin Hall conductivity (SHC) σ_{xy}^z, defined via $J_x^z = \hbar j_x^z/2 = \hbar(v_x\sigma_z + \sigma_z v_x)/4 = \sigma_{xy}^z E_y$, where v_x is the x component of the velocity operator and $\sigma_{x,y,z}$ are the Pauli matrices, for a p-doped three-dimensional (bulk) valence-band system[3] and for a two-dimensional electron gas (2DEG) with the Rashba spin-orbit interaction.[4]

A number of theoretical papers have investigated the robustness of the ballistic SHC σ_{xy}^z as arising from the intrinsic mechanism, against scattering by nonmagnetic[5–11] and magnetic[12] impurities, its dependence on specific classes of SO interactions,[10] and the interplay between the SO coupling and magnetic fields.[11,13,14] Two early experimental efforts[15,16] have probed the spin Hall effect for electrons and holes.[17] Kato *et al.*[15] find that the SHE in n-GaAs epilayers is due to the extrinsic mechanism (nonmagnetic impurities) while Wunderlich *et al.*[16] conclude that the SHE in the 2D hole gas probed in their experiment is intrinsic. Further investigations have also shown that the SHE in 2DEGs is of the extrinsic type.[18]

Following an early debate concerning the robustness of the intrinsic SHE, it is now well established that the dc SHC

as defined above vanishes identically for model Hamiltonians with a linear-in-the-carrier-momentum SO interaction, such as that of Rashba[13] and/or the linearized Dresselhaus. This holds in both the ballistic case ("clean limit") and in the limit of weak scattering by nonmagnetic impurities.[5–11,19] This result can be understood by examining the relationship between the time derivative of the spin density and spin current in these systems. As pointed out in Refs. 8, 9, and 20, for Rashba-type models $d\sigma_k/dt \propto j_k^z$, $k=x,y$ and should vanish in the dc steady-state regime (in the presence of some relaxation mechanism) where $d\sigma_k/dt=0$.[21]

The search for new materials that can exhibit the SHE as well as other types of SO interactions has continued over the years.[22] Recently, we have introduced a type of SO interaction present in III-V (or II-VI) zinc-blende semiconductor quantum wells with more than one subband.[23,24] This intersubband-induced SO term is similar in form to the Rashba SO interaction. However, it couples electron states from distinct subbands and hence can be nonzero even in structurally symmetric wells. For an electron in a symmetric quantum well with two subbands we have[23,24]

$$\mathcal{H} = \left(\frac{\mathbf{p}^2}{2m} + \overline{\mathcal{E}}\right)\mathbb{1}\otimes\mathbb{1} - \frac{\Delta\mathcal{E}}{2}\tau_z\otimes\mathbb{1} + \frac{\eta}{\hbar}\tau_x\otimes(p_x\sigma_y - p_y\sigma_x),$$

$$(1)$$

where m is the effective mass, $\overline{\mathcal{E}}=(\mathcal{E}_e+\mathcal{E}_o)/2$ and $\Delta\mathcal{E}=\mathcal{E}_o - \mathcal{E}_e$, with $\mathcal{E}_e$ and $\mathcal{E}_o$ denoting the band edges of the lowest (even) and first excited (odd) subbands. $\tau_{x,y,z}$ and $\sigma_{x,y,z}$ are Pauli matrices describing the subband degree of freedom and the electron spin, respectively. The intersubband-induced SO coupling η depends on the structural potential of the well, the electronic Hartree potential, and the external gate potential.[24]

In this paper we calculate the dc spin Hall conductivity σ_{xy}^z for 2D electrons in the presence of the intersubband-induced SO interaction in wells with two subbands. We use the Kubo formula in the ballistic limit. We follow Rashba's approach[13] by performing our calculation in the presence of a perpendicular magnetic field B, which modifies the energy spectrum (Landau levels) thus allowing us to consistently

include intrabranch and interbranch transitions in the Kubo formula, and then taking the $B \to 0$ limit. With this procedure, known to produce the correct vanishing of σ_{xy}^z for the Rashba model,[13] we derive an analytical expression for the dc SHC in two subband systems. More specifically, we find that: (i) σ_{xy}^z is nonzero for electrons whose Fermi energy $\mathcal{E}_F$ lies between the subband edges $\mathcal{E}_e$ and $\mathcal{E}_o$, i.e., when only the lowest subband is occupied, and (ii) σ_{xy}^z is null for $\mathcal{E}_F > \mathcal{E}_o$, i.e., when two subbands are occupied. Interestingly, the nonzero SHC is nonuniversal (e.g., it depends on η), exhibits a nonmonotonic behavior and a sign change for $\mathcal{E}_e < \mathcal{E}_F < \mathcal{E}_o$. In addition, the SHC presents finite jumps at the subband edges when plotted as a function of $\mathcal{E}_F$ (or the carrier areal density n_{2D}) due to discontinuities in the density of states (DOS) contributing to the spin density. We have also performed a detailed self-consistent calculation of the energy spectrum and wave functions for realistic wells, from which we determine η and the corresponding σ_{xy}^z. The magnitude of our self-consistently determined SHC is, however, much smaller than $\sigma_0 = e/4\pi$.[25]

Before describing in detail our linear-response calculation for the SHC, here we present a simple argument as to why we could expect a nonvanishing SHC for electrons in 2DEGs with two subbands where the intersubband SO interaction is operative. Despite the formal similarity between the SO term in our Hamiltonian, Eq. (1) and that of Rashba, here we find a different relationship between the spin current and spin density, i.e.,

$$j_x^z = \frac{\hbar^2}{2m\eta}\left[\frac{d}{dt}(\tau_x \otimes \sigma_x) - \frac{\Delta\mathcal{E}}{\hbar}\tau_y \otimes \sigma_x\right], \quad (2)$$

in contrast to the Rashba model for which $d\sigma_x/dt \propto j_x^z$. In Eq. (2) the spin current is related to the subband-related spin densities $\tau_x \otimes \sigma_x$ and $\tau_y \otimes \sigma_x$. The second term in Eq. (2), absent in the Rashba system, suggests that the (pseudo) spin-density response to an applied electric field can contribute to the spin current—even in the dc steady-state limit where $d(\tau_x \otimes \sigma_x)/dt = 0$. Hence, 2DEGs formed in two subband wells with intersubband SO coupling may have a nonzero SHC. Our detailed linear-response calculation below shows that this is indeed the case in the clean limit.

II. MODEL HAMILTONIAN AND KUBO FORMULA

Let us consider our Hamiltonian (1) in the presence of a magnetic field $B\hat{z} = \nabla \times \mathbf{A}$ by making the replacement $\mathbf{p} \to \boldsymbol{\pi} = \mathbf{p} - (e/c)\mathbf{A}$. For simplicity, we do not consider the Zeeman splitting (i.e., we assume a zero g factor[14]). Since our SO term couples only electrons with opposite spins in different subbands, the subband-spin Hilbert space $\{|bs\rangle; b = e, o, s = \uparrow, \downarrow\}$ can be divided into two independent subspaces $\mathcal{F}_+ = \{|e\uparrow\rangle, |o\downarrow\rangle\}$ and $\mathcal{F}_- = \{|o\uparrow\rangle, |e\downarrow\rangle\}$, and the 2×2 Hamiltonian in each subspace $\lambda = \pm$ can be written as

$$\mathcal{H}_\lambda = \frac{\boldsymbol{\pi}^2}{2m} + \overline{\mathcal{E}} - \begin{bmatrix} \lambda\Delta\mathcal{E}/2 & \eta(\pi_y + i\pi_x)/\hbar \\ \eta(\pi_y - i\pi_x)/\hbar & -\lambda\Delta\mathcal{E}/2 \end{bmatrix}. \quad (3)$$

The reduced Hamiltonian is identical to that of a 2DEG with a Rashba SO coupling of strength η and an effective Zeeman

splitting $\lambda\Delta\mathcal{E}$. Note that only the sign of the effective Zeeman splitting differs between $\mathcal{H}_\lambda$ in two subspaces.

In the absence of the SO coupling ($\eta = 0$), the Schrödinger equation gives rise to the Landau levels $|bsn\rangle_0$ with the level index $n \geq 0$ for each subband b and spin s. The Landau levels are evenly spaced by the cyclotron gap $\hbar\omega_c = |eB|/mc$. The degeneracy (per unit volume) of each level and the magnetic length are, respectively, $1/2\pi l^2$ and $l = \sqrt{c\hbar/eB}$. For nonzero SO coupling ($\eta \neq 0$) the coupling of Landau levels within the same subspace produces the mixed Landau levels $|\lambda\mu n\rangle$,

$$\begin{bmatrix} |\lambda + n\rangle \\ |\lambda - n\rangle \end{bmatrix} = \begin{bmatrix} \sin\dfrac{\theta_{\lambda n}}{2} & -i\cos\dfrac{\theta_{\lambda n}}{2} \\ \cos\dfrac{\theta_{\lambda n}}{2} & -i\sin\dfrac{\theta_{\lambda n}}{2} \end{bmatrix} \begin{bmatrix} |b_1\uparrow n\rangle_0 \\ |b_2\downarrow n-1\rangle_0 \end{bmatrix}, \quad (4)$$

where $(b_1, b_2) = (e, o)$ for $\lambda = +$ and (o, e) for $\lambda = -$, with the corresponding eigenenergies

$$\mathcal{E}_{\lambda\mu n} = \overline{\mathcal{E}} + \hbar\omega_c(n - \mu\gamma_{\lambda n}). \quad (5)$$

Here $\mu = \pm$ denotes the spin branch. It is convenient to introduce dimensionless parameters $\mathcal{E}_{so} = 2m\eta^2/\hbar^3\omega_c$ and $\mathcal{E}_g = \Delta\mathcal{E}/\hbar\omega_c$ for the SO coupling energy and the subband gap, respectively. In term of these we can define $\sin\theta_{\lambda n} = \sqrt{n\mathcal{E}_{so}}/\gamma_{\lambda n}$ and $\cos\theta_{\lambda n} = \zeta_\lambda/\gamma_{\lambda n}$ with $\zeta_\lambda = (1 - \lambda\mathcal{E}_g)/2$ and $\gamma_{\lambda n} = \sqrt{n\mathcal{E}_{so} + \zeta_\lambda^2}$. Note that the eigenstate for $n = 0$ exists only for $\mu = -\text{sgn}\,\zeta_\lambda$.

We determine the dc spin Hall conductivity at zero temperature by using the Kubo formula[13]

$$\sigma_{xy}^z = -\frac{ie}{2\pi l^2}\sum_\lambda \sum_{\mu n\mu' n'}' \frac{\langle\lambda\mu n|j_x^z|\lambda\mu' n'\rangle\langle\lambda\mu' n'|v_y|\lambda\mu n\rangle}{(\omega_{\lambda\mu n} - \omega_{\lambda\mu' n'})^2}, \quad (6)$$

where the primed sum indicates that it should be performed over the states with $\omega_{\lambda\mu n} = \mathcal{E}_{\lambda\mu n}/\hbar < \mathcal{E}_F/\hbar$ and $\omega_{\lambda\mu' n'} > \mathcal{E}_F/\hbar$. Here we have used the fact that the operators j_x^z and v_y couple only states in same subspace and the matrices $\langle\lambda\mu n|j_x^z|\lambda\mu' n'\rangle$ and $\langle\lambda\mu' n'|v_y|\lambda\mu n\rangle$ are symmetric and antisymmetric, respectively. Since the matrix elements are independent of the guiding center position, the factor $1/2\pi l^2$ appears due to the Landau-level degeneracy.

A more insightful analysis of the SHC can be achieved by expressing the operators in terms of commutators with the Hamiltonian. First, the relation $v_y = (i/\hbar)[\mathcal{H}, y]$ leads to

$$\langle\lambda\mu' n'|v_y|\lambda\mu n\rangle = il^2(\omega_{\lambda\mu' n'} - \omega_{\lambda\mu n})\langle\lambda\mu' n'|k_x|\lambda\mu n\rangle, \quad (7)$$

with $k_x = (a^\dagger + a)/\sqrt{2}l$. This is a direct consequence of the definition of the ladder operator $a = (l/\sqrt{2}\hbar)(\pi_x + i\pi_y) = (y + l^2 p_x/\hbar + il^2 p_y/\hbar)/\sqrt{2}l$. From Eq. (2), on the other hand, we can obtain

$$\langle\lambda\mu n|j_x^z|\lambda\mu' n'\rangle = -\frac{\hbar\Delta\mathcal{E}}{2m\eta}\langle\lambda\mu n|\tau_y \otimes \sigma_x|\lambda\mu' n'\rangle$$

$$+ \frac{i\hbar^2}{2m\eta}(\omega_{\lambda\mu n} - \omega_{\lambda\mu' n'})$$

$$\times \langle\lambda\mu n|\tau_x \otimes \sigma_x|\lambda\mu' n'\rangle. \quad (8)$$
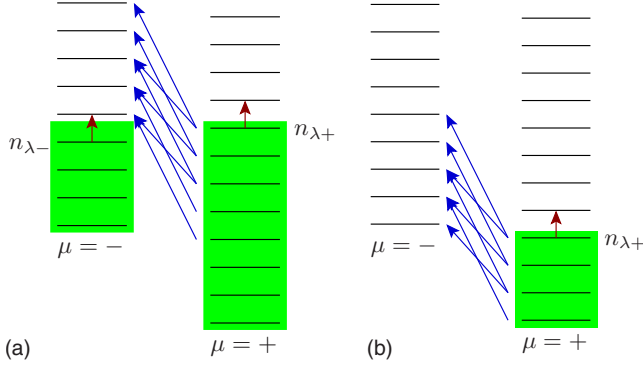
FIG. 1. (Color online) Diagrams describing the interbranch (long arrows) and intrabranch (short arrows) transitions. (a) Left and (b) right panels correspond to the cases $\mathcal{E}_F > \mathcal{E}_o$ and $\mathcal{E}_e < \mathcal{E}_F < \mathcal{E}_o$, respectively. $n_\pm$ denotes the highest-filled Landau level in the spin branch μ.

Substitution of Eqs. (7) and (8) into Eq. (6) gives rise to $\sigma_{xy}^z = \sigma^{(1)} + \sigma^{(2)}$, with

$$\frac{\sigma^{(1)}}{\sigma_0} = \sum_\lambda \sideset{}{'}\sum_{\mu n \mu' n'} \frac{\hbar^2}{im\eta} \langle \lambda \mu n | \tau_x \otimes \sigma_x | \lambda \mu' n' \rangle \langle \lambda \mu' n' | k_x | \lambda \mu n \rangle, \tag{9a}$$

$$\frac{\sigma^{(2)}}{\sigma_0} = \sum_\lambda \sideset{}{'}\sum_{\mu n \mu' n'} \frac{\hbar \Delta \mathcal{E}}{m \eta} \frac{\langle \lambda \mu n | \tau_y \otimes \sigma_x | \lambda \mu' n' \rangle \langle \lambda \mu' n' | k_x | \lambda \mu n \rangle}{\omega_{\lambda \mu n} - \omega_{\lambda \mu' n'}}, \tag{9b}$$

with $\sigma_0 \equiv e/4\pi$.[25] Each of the two terms can be further divided into two contributions coming from two different transitions classified by the restriction on the spin branches of states to be summed over: interbranch and intrabranch transitions.[13]

As can be seen from Fig. 1, the interbranch contributions describe transitions from the filled states in the lower branch $\mu = +$ to the empty ones in the upper branch $\mu = -$ and follow the selection rule $|\lambda + n\rangle \rightarrow |\lambda - n \pm 1\rangle$. The intrabranch transitions are possible only in the vicinity of the Fermi level in each spin branch and obey a similar selection rule $|\lambda \mu n_{\lambda \mu}\rangle \rightarrow |\lambda \mu n_{\lambda \mu} + 1\rangle$, where $n_{\lambda \mu}$ is the index of the highest-filled Landau level in the subspace λ and spin branch μ; see Fig. 1. In what follows, we write $\sigma^{(i)} = \sigma_{\text{inter}}^{(i)} + \sigma_{\text{intra}}^{(i)}$ with $i = 1, 2$ to identify and separately investigate the contributions from the interbranch and intrabranch transitions.

III. SPIN HALL CONDUCTIVITY

First we investigate $\sigma^{(1)}$. Making use of the fact that the matrices $\langle \lambda \mu n | \tau_x \otimes \sigma_x | \lambda \mu' n' \rangle$ and $\langle \lambda \mu' n' | k_x | \lambda \mu n \rangle$ are antisymmetric and symmetric, respectively, one can derive the two following identities

$$\sideset{}{^*}\sum_{n \mu n' \mu'} \langle \lambda \mu n | \tau_x \otimes \sigma_x | \lambda \mu' n' \rangle \langle \lambda \mu' n' | k_x | \lambda \mu n \rangle = 0, \tag{10a}$$

$$\sum_{n' \mu'} \langle \lambda \mu n | \tau_x \otimes \sigma_x | \lambda \mu' n' \rangle \langle \lambda \mu' n' | k_x | \lambda \mu n \rangle = 0, \tag{10b}$$

where the asterisk over the sum indicates that it should be done over the states with $\mathcal{E}_{n\mu}, \mathcal{E}_{n'\mu'} < \mathcal{E}_F$. We have used the commutation relation $[\tau_x \otimes \sigma_x, k_x] = 0$ to prove the second identity, which is valid for arbitrary λ, μ, and n. Applying these identities to Eq. (9a) reveals that $\sigma^{(1)}$ vanishes identically for arbitrary B and $\mathcal{E}_F$. Interestingly, the interbranch and intrabranch contributions exactly cancel out, i.e., $\sigma_{\text{inter}}^{(1)} = -\sigma_{\text{intra}}^{(1)}$. This cancellation is similar to that which occurs in the Rashba model.[13] Here, however, the extended operator $\tau_x \otimes \sigma_x$ replaces the spin operator σ_x in the Rashba case. More explicitly, we have

$$\frac{\sigma_{\text{inter}}^{(1)}}{\sigma_0} = -\frac{\sigma_{\text{intra}}^{(1)}}{\sigma_0} = \frac{1}{2} \sum_\lambda \begin{cases} \dfrac{n_{\lambda+}}{\gamma_{n_{\lambda+}}} - \dfrac{n_{\lambda-} + 1}{\gamma_{n_{\lambda-}+1}}, & \mathcal{E}_F > \mathcal{E}_o, \\[3mm] \dfrac{n_{\lambda+}}{\gamma_{n_{\lambda+}}}, & \mathcal{E}_e < \mathcal{E}_F < \mathcal{E}_o. \end{cases} \tag{11}$$

In the $B \rightarrow 0$ limit, we obtain

$$\frac{\sigma_{\text{inter}}^{(1)}}{\sigma_0} = -\frac{\sigma_{\text{intra}}^{(1)}}{\sigma_0} = \begin{cases} \dfrac{\kappa_1 \kappa_2 + 1/2}{\kappa_1 \kappa_2 + 1/4}, & \mathcal{E}_F > \mathcal{E}_o, \\[3mm] 1 + \dfrac{\kappa_2}{\kappa_3 + \kappa_1/2}, & \mathcal{E}_e < \mathcal{E}_F < \mathcal{E}_o \end{cases} \tag{12}$$

with $\kappa_1 = \mathcal{E}_{\text{so}}/\mathcal{E}_g$, $\kappa_2 = (\mathcal{E}_F - \bar{\mathcal{E}})/\Delta \mathcal{E}$, and $\kappa_3 = \sqrt{\kappa_1^2/4 + \kappa_1 \kappa_2 + 1/4}$. It is worth noting that $\sigma_{\text{intra}}^{(1)}$ (or $\sigma_{\text{inter}}^{(1)}$) varies continuously as $\mathcal{E}_F$ passes through the upper subband energy edge $\mathcal{E}_o$, even though the intrabranch transitions coming from the $\mu = -$ spin branch [see Fig. 1(b)] stop contributing at this energy. This is so because the contribution $(n_{\lambda-} + 1)/\gamma_{n_{\lambda-}+1}$ in Eq. (11) vanishes as $\mathcal{E}_F \rightarrow \mathcal{E}_o$.

We now evaluate the second term $\sigma^{(2)}$ of the spin Hall conductivity, Eq. (9b). In our model, $\sigma^{(2)}$ arises solely from the pseudospin density response [see Eq. (2)], which has no counterpart in the Rashba model. Differently than $\sigma^{(1)}$, the expression for $\sigma^{(2)}$ contains a factor $\omega_{\lambda \mu n} - \omega_{\lambda \mu' n'}$ in the denominator [cf., Eqs. (9a) and (9b)]; this prevents us from deriving identities such as Eq. (10) for $\sigma^{(2)}$. Hence, no exact cancellation between the interbranch and intrabranch contributions is guaranteed for $\sigma^{(2)}$. In general, $\sigma^{(2)}$ is nonzero for arbitrary B. In addition, the denominator factor in $\sigma^{(2)}$ allows for the possibility of a finite contribution to $\sigma^{(2)}$ even if the matrix elements in the numerator of Eq. (9b) vanish, provided that $(\omega_{\lambda \mu n} - \omega_{\lambda \mu' n'})$ goes to zero as well. This, in contrast to the $\sigma^{(1)}$ case, makes the intrabranch contribution $\sigma_{\text{intra}}^{(2)}$ discontinuous as $\mathcal{E}_F$ crosses the subband edges.

Explicitly, the interbranch and intrabranch contributions to $\sigma^{(2)}$ are

$$\frac{\sigma_{\text{inter}}^{(2)}}{\sigma_0} = \sum_\lambda \frac{\lambda}{2} \mathcal{E}_g \sum_{n=\max(n_{\lambda-}+1,0)}^{n_{\lambda+}-1} \frac{\dfrac{n+1+\zeta_\lambda}{\gamma_{\lambda n+1}} - \dfrac{n-\zeta_\lambda}{\gamma_{\lambda n}}}{(\gamma_{\lambda n+1}+\gamma_{\lambda n})^2 - 1}, \tag{13a}$$

$$\frac{\sigma_{\text{intra}}^{(2)}}{\sigma_0} = \sum_\lambda \frac{\lambda}{2} \mathcal{E}_g \begin{cases} \dfrac{2n_{\lambda+}+1+\dfrac{n_{\lambda+}-\zeta_\lambda}{\gamma_{\lambda n_{\lambda+}}}}{1-\mathcal{E}_{\text{so}}+2\gamma_{\lambda n_{\lambda+}}} - \dfrac{2n_{\lambda-}+1+\dfrac{n_{\lambda-}+1+\zeta_\lambda}{\gamma_{\lambda n_{\lambda-}+1}}}{1+\mathcal{E}_{\text{so}}+2\gamma_{\lambda n_{\lambda-}+1}}, & \mathcal{E}_F > \mathcal{E}_o, \\[4ex] \dfrac{2n_{\lambda+}+1+\dfrac{n_{\lambda+}-\zeta_\lambda}{\gamma_{\lambda n_{\lambda+}}}}{1-\mathcal{E}_{\text{so}}+2\gamma_{\lambda n_{\lambda+}}}, & \mathcal{E}_e < \mathcal{E}_F < \mathcal{E}_o. \end{cases} \tag{13b}$$

The intrabranch contribution from the $\mu=-$ spin branch, i.e., the second term in Eq. (13b), present only for $\mathcal{E}_F > \mathcal{E}_o$, does not vanish as $\mathcal{E}_F \to \mathcal{E}_o$ and $B \to 0$. This leads to a discontinuity in $\sigma^{(2)}$ at $\mathcal{E}_F = \mathcal{E}_o$. A similar discontinuity occurs at $\mathcal{E}_F = \mathcal{E}_e$ due to the first term in Eq. (13b) not vanishing as $\mathcal{E}_F \to \mathcal{E}_e$ and $B \to 0$. In the $B \to 0$ limit, Eq. (13) simplifies to

$$\frac{\sigma_{\text{inter}}^{(2)}}{\sigma_0} = \begin{cases} -\dfrac{1}{2\kappa_1\kappa_2+1/2}, & \mathcal{E}_F > \mathcal{E}_o, \\[2ex] \dfrac{1}{\kappa_1}\left(\dfrac{1}{2\kappa_3+\kappa_1}-1\right), & \mathcal{E}_e < \mathcal{E}_F < \mathcal{E}_o, \end{cases} \tag{14a}$$

$$\frac{\sigma_{\text{intra}}^{(2)}}{\sigma_0} = \begin{cases} \dfrac{1}{2\kappa_1\kappa_2+1/2}, & \mathcal{E}_F > \mathcal{E}_o, \\[2ex] \dfrac{1}{2\kappa_3(2\kappa_3+\kappa_1)}+\dfrac{\kappa_2+\kappa_1/2}{4\kappa_3^3}, & \mathcal{E}_e < \mathcal{E}_F < \mathcal{E}_o. \end{cases} \tag{14b}$$

Interestingly, the above results show that the interbranch and intrabranch contributions to $\sigma^{(2)}$ exactly cancel out in the B

FIG. 2. (Color online) Self-consistent potential profile of our InSb/Al$_{0.3}$In$_{0.7}$Sb quantum well with two subbands. The calculated subband edges $\mathcal{E}_e=1.0$ meV and $\mathcal{E}_o=187.3$ meV and the corresponding wave functions are also shown. The Fermi energy is $\mathcal{E}_F=100.3$ meV.

$\to 0$ limit, provided that $\mathcal{E}_F > \mathcal{E}_o$, i.e., when both spin branches are filled. Note that this cancellation only occurs in the $B \to 0$ limit. Hence, since $\sigma^{(1)}$ identically vanishes for any $\mathcal{E}_F$ and B, we find that in the $B \to 0$ limit σ_{xy}^z is nonvanishing only for $\mathcal{E}_e < \mathcal{E}_F < \mathcal{E}_o$ being given by

$$\sigma_{xy}^z = \sigma^{(2)} = \sigma_0\left[\frac{1}{\kappa_1}\left(\frac{1}{2\kappa_3}-1\right)+\frac{\kappa_2+\kappa_1/2}{4\kappa_3^3}\right]. \tag{15}$$

In the above expressions, the Fermi energy $\mathcal{E}_F$ (at $B=0$) is given by

$$\mathcal{E}_F = \begin{cases} \dfrac{\pi\hbar^2 n_{2D}}{2m} + \bar{\mathcal{E}} + \dfrac{m\eta^2}{\hbar^2}, & \mathcal{E}_F > \mathcal{E}_o \\[3ex] \dfrac{\pi\hbar^2 n_{2D}}{m\left(1+\dfrac{2m\eta^2}{\hbar^2\Delta\mathcal{E}}\right)} + \mathcal{E}_e, & \mathcal{E}_e < \mathcal{E}_F < \mathcal{E}_o \end{cases} \tag{16}$$

as can be straightforwardly derived from the $B=0$ spectrum of our system.[26] Next we calculate σ_{xy}^z for realistic wells.

IV. SELF-CONSISTENT CALCULATION AND RESULTS

We have performed a detailed self-consistent calculation—by solving the Schrödinger and Poisson's equations in the Hartree approximation—to determine the intersubband SO coupling strength η for realistic symmetric wells[24] and the corresponding spin Hall conductivity $\sigma_{xy}^z(\eta)$. We have considered a modulation-doped symmetric Al$_{0.3}$In$_{0.7}$Sb/InSb/Al$_{0.3}$In$_{0.7}$Sb quantum well with only two subbands;[27] see Fig. 2. The structure comprises a single well of width $L_w=15$ nm and two n-doped semi-infinite adjacent regions. We assume that the ionized impurities giving up electrons to the well form a continuum positive background with density ρ of width $w=5$ nm (depletion layer). Our self-consistent calculation follows that of Ref. 24.

In an earlier work,[24] we have found that narrow single InSb wells give sizable values for the intersubband-induced SO coupling strength η. Here we self-consistently calculate the corresponding spin Hall conductivity as a function of the areal density n_{2D}.[28] Figure 3 shows the calculated inter-
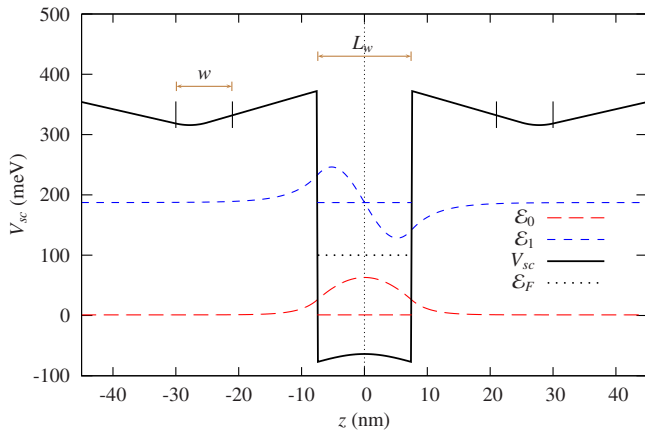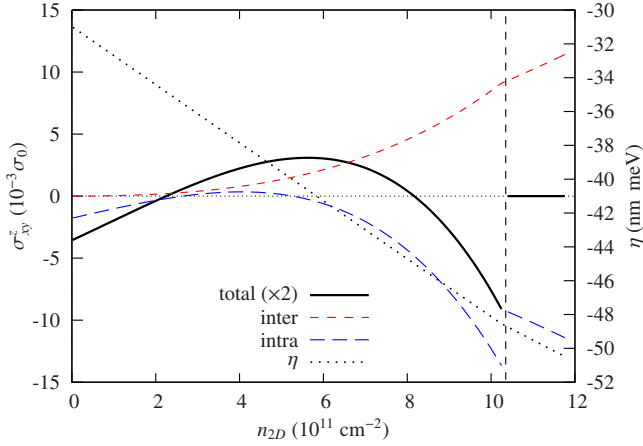
FIG. 3. (Color online) Interbranch (dashed line) and intrabranch (long-dashed line) conductivity contributions and the total (solid line) spin Hall conductivity σ_{xy}^z (in units of $\sigma_0 = e/4\pi$) as functions of the areal density n_{2D} in the single InSb well shown in Fig. 2. Note the discontinuities at $\mathcal{E}_F = \mathcal{E}_o$ and $\mathcal{E}_F = \mathcal{E}_e$, which correspond to $n_{2D} = 10.3 \times 10^{11}$ cm^{-2} and $n_{2D} = 0$, respectively.

branch $(\sigma_{\text{inter}} = \sigma_{\text{inter}}^{(1)} + \sigma_{\text{inter}}^{(2)})$ and intrabranch $(\sigma_{\text{intra}} = \sigma_{\text{intra}}^{(1)} + \sigma_{\text{intra}}^{(2)})$ conductivity contributions and the total spin Hall conductivity σ_{xy}^z [see Eq. (15)] as a function of the areal density n_{2D} (or $\mathcal{E}_F$) for a single InSb well. Note the two discontinuities of the SHC at densities corresponding to $\mathcal{E}_F = \mathcal{E}_o$ (see vertical dashed line) and $\mathcal{E}_F = \mathcal{E}_e$ (at $n_{2D} = 0$). The magnitude of these jumps are $\Delta\sigma/\sigma_0 = \kappa_1/(1 + \kappa_1)^2$ and $-\kappa_1/(1 - \kappa_1)^2$, respectively. These discontinuities come from the intrabranch contribution $\sigma_{xy,\text{intra}}^z = \sigma_{\text{intra}}^{(2)}$ while the interbranch contribution $\sigma_{xy,\text{inter}}^z = \sigma_{\text{inter}}^{(2)}$ varies smoothly with $\mathcal{E}_F$ (recall that $\sigma^{(1)} = 0$). In addition, the competition between $\sigma_{\text{intra}}^{(2)}$ and $\sigma_{\text{inter}}^{(2)}$ can lead to a sign change in σ_{xy}^z as $\mathcal{E}_F$ is varied, see Fig. 3. It should be noted that as the strength of the SO coupling η (or κ_1) becomes smaller, $\Delta\sigma$ and σ_{xy}^z diminish as well, thus vanishing completely at $\kappa_1 = 0$. Despite the interesting features displayed by the total spin Hall conductivity—the sign change and the nonmonotonic behavior—as the electron density is varied between the subband edges, we find that the largest values of σ_{xy}^z are extremely small ($\sim 10^{-3}\sigma_0$).

V. ADDITIONAL DISCUSSION

Considering the formal similarity between our Hamiltonian containing the intersubband-induced SO coupling and Rashba's, it is not entirely surprising that the SHC vanishes when both spin branches are filled. Novel effects of the intersubband-induced SO term arise when only the lower branch is filled: an incomplete cancellation between the contributions from the interbranch and intrabranch transitions lead to a nonzero SHC and discontinuities in it. The origin of these discontinuities can be traced back to the abrupt changes in $B = 0$ DOS of the model at the subband edges. The $B = 0$ DOS for each spin branch is given by $\rho_{\mp} = \frac{1}{2}\rho_0(1 \mp \kappa_1/2\kappa_3)$ with $\rho_0 = m/\pi\hbar^2$. Hence the DOS abruptly changes at $\mathcal{E}_F = \mathcal{E}_o$ from a constant value $\rho_+ + \rho_- = \rho_0$ to ρ_+, thus giving rise to an abrupt loss of states contributing to the spin-density

response. In fact, the intrabranch contribution, that is, responsible for the discontinuity is proportional to the DOS, that is, $1/(\omega_{\lambda\mu n_{\lambda\mu}} - \omega_{\lambda\mu n_{\lambda\mu}+1}) \propto \rho_\mu$ [see Eq. (9b)]. The discontinuity $\Delta\sigma$ in σ_{xy}^z can be explicitly related to the discontinuity $\Delta\rho$ in the DOS as follows:

$$\frac{\Delta\sigma}{\sigma_0} = \begin{cases} 2\dfrac{\Delta\rho}{\rho_0}\left(1 - 2\dfrac{\Delta\rho}{\rho_0}\right), & \mathcal{E}_F = \mathcal{E}_o \\ -2\dfrac{\Delta\rho}{\rho_0}\left(1 + 2\dfrac{\Delta\rho}{\rho_0}\right), & \mathcal{E}_F = \mathcal{E}_e. \end{cases} \quad (17)$$

Note that both expressions vanish as $\Delta\rho/\rho_0 \to 0$, clearly showing that $\Delta\sigma$ arises from the discontinuity in the DOS.

Our intersubband-induced SO coupling mixes both the spin and the subband degrees of freedom simultaneously. Therefore it does not provide a mechanism to couple *opposite* spins within a given subband. This implies that any projection of our Hamiltonian into the lower subband, in the limit of large subband gap $\Delta\mathcal{E} \gg \mathcal{E}_{\text{so}}$, would not produce an effective SO coupling between spins within the lower subband so that no finite SHC appears. This limiting case study stresses that our finite SHC, even for Fermi energies near the lower subband bottom, is due to the subband-transfer process, even though it should be quite small in the limit $\Delta\mathcal{E} \gg \mathcal{E}_{\text{so}}$. We expect, however, that additional subband mixing but spin-preserving scattering mechanisms, such as impurity scattering, can induce an effective SO coupling within a given subband when mediated by the intersubband-induced SO coupling, which mixes both spins and subbands. This impurity-mediated SO coupling may then affect and possibly even enhance the strength of the SHC, as long as its momentum randomization is weak enough.

As a final point we mention that interbranch contribution $\sigma_{xy,\text{inter}}^z$ reproduces the result for the SHC calculated via the Kubo formula in the absence of a magnetic field. Note that this quantity is nonuniversal and vanishes as $\eta \to 0$. Nevertheless, we stress that it alone does not constitute the total SHC.

VI. SUMMARY AND FINAL REMARKS

We have calculated the ballistic spin Hall conductivity σ_{xy}^z for symmetric wells with two subbands in which the intersubband-induced SO interaction is present. We follow a linear-response approach due to Rashba which consistently accounts for intrabranch and interbranch transitions in the Kubo formula. We find that σ_{xy}^z is zero when the two subbands are occupied (similar to the Rashba model) and nonzero when only the lower subband is occupied. We have also performed a numerical self-consistent calculation to determine the intersubband SO strength for realistic InSb wells and have calculated the corresponding σ_{xy}^z. Even though the calculated σ_{xy}^z shows interesting features such as discontinuities at the subband edges (due to discontinuities in the DOS), a nonmonotonic behavior and a sign change as a function of the Fermi energy (or areal density), the magnitude of σ_{xy}^z is much smaller than 1 in units of $e/4\pi$.

It is conceivable that other materials systems, e.g., metallic surfaces and interfaces, can display intersubband-induced

SO interaction, in addition to the usual Rashba. For instance, metallic surfaces with unconventional spin topology[29] where deviations from the usual Rashba model have recently been reported (and for which the SO couplings are much stronger than in semiconductors) are a possibility. Perhaps in these systems the SHC due to the intersubband SO coupling would be sizable.

One caveat of our calculation is that we use a spin-current definition which is a simple extension for two subbands of the conventional (not uniquely defined[30]) symmetrized product of the spin and velocity operators as in Rashba model. Hence all the issues related to the reality of these currents and whether or not they would lead to spin accumulation in finite samples appear here as well. More work is certainly needed to address these issues.[31] Using nonequilibrium

Green's functions on a lattice, we have performed some simulations[32] of the spin density in bilayer systems with interlayer SO orbit coupling, whose Hamiltonian maps onto our two-subband one. Our preliminary results show that the spin density changes as compared to the single-layer case (Rashba model). Finally, we emphasize that the role of impurities, which we believe should not kill the effect discussed here, remains an interesting problem for further investigations.

[1] For reviews, see H.-A. Engel, E. I. Rashba, and B. I. Halperin, *Handbook of Magnetism and Advanced Magnetic Materials* (John Wiley & Sons, Chichester, 2007); and J. Schliemann, Int. J. Mod. Phys. B **20**, 1015 (2006).

[2] M. I. Dyakonov and V. I. Perel, Zh. Eksp. Teor. Fiz. Pis'ma Red. **13**, 657 (1971) [JETP Lett. **13**, 467 (1971)]; J. E. Hirsch, Phys. Rev. Lett. **83**, 1834 (1999); S. Zhang, *ibid.* **85**, 393 (2000); L. Hu, J. Gao, and S.-Q. Shen, Phys. Rev. B **68**, 115302 (2003); M. I. Dyakonov, Phys. Rev. Lett. **99**, 126601 (2007).

[3] S. Murakami, N. Nagaosa, and S. C. Zhang, Science **301**, 1348 (2003); Phys. Rev. B **69**, 235206 (2004).

[4] J. Sinova, D. Culcer, Q. Niu, N. A. Sinitsyn, T. Jungwirth, and A. H. MacDonald, Phys. Rev. Lett. **92**, 126603 (2004).

[5] J. I. Inoue, G. E. W. Bauer, and L. W. Molenkamp, Phys. Rev. B **70**, 041303(R) (2004).

[6] E. G. Mishchenko, A. V. Shytov, and B. I. Halperin, Phys. Rev. Lett. **93**, 226602 (2004).

[7] R. Raimondi and P. Schwab, Phys. Rev. B **71**, 033311 (2005).

[8] O. Chalaev and D. Loss, Phys. Rev. B **71**, 245318 (2005).

[9] O. V. Dimitrova, Phys. Rev. B **71**, 245327 (2005).

[10] A. G. Mal'shukov and K. A. Chao, Phys. Rev. B **71**, 121308(R) (2005).

[11] S.-Q. Shen, M. Ma, X. C. Xie, and F. C. Zhang, Phys. Rev. Lett. **92**, 256603 (2004); S.-Q. Shen, Y.-J. Bao, M. Ma, X. C. Xie, and F. C. Zhang, Phys. Rev. B **71**, 155316 (2005).

[12] C. Gorini, P. Schwab, M. Dzierzawa, and R. Raimondi, Phys. Rev. B **78**, 125327 (2008).

[13] E. I. Rashba, Phys. Rev. B **70**, 201309(R) (2004).

[14] P. Lucignano, R. Raimondi, and A. Tagliacozzo, Phys. Rev. B **78**, 035336 (2008).

[15] Y. K. Kato, R. C. Myers, A. C. Gossard, and D. D. Awschalom, Science **306**, 1910 (2004); N. P. Stern, D. W. Steuerman, S. Mack, A. C. Gossard, and D. D. Awschalom, Nat. Phys. **4**, 843 (2008).

[16] J. Wunderlich, B. Kaestner, J. Sinova, and T. Jungwirth, Phys. Rev. Lett. **94**, 047204 (2005).

[17] J. Schliemann and D. Loss, Phys. Rev. B **71**, 085308 (2005).

[18] V. Sih, R. C. Myers, Y. K. Kato, W. H. Lau, A. C. Gossard, and D. D. Awschalom, Nat. Phys. **1**, 31 (2005).

[19] J. Sinova, S. Murakami, S.-Q. Shen, and M.-S. Choi, Solid State Commun. **138**, 214 (2006).

[20] S. I. Erlingsson, J. Schliemann, and D. Loss, Phys. Rev. B **71**, 035319 (2005).

[21] We note, however, that finite-size effects and quantum interference can still lead to coherent spin accumulation or nontrivial spin conductance, provided that the sample size is comparable to the spin precession length (Refs. 33–36). Moreover, for oscillating driving fields (Ref. 37) electron-spin-resonance-type phenomenon is possible in Rashba-coupled 2DEGs in the presence of an in-plane magnetic field and a nonzero SHC emerges in the high-frequency (as compared to the inverse momentum relaxation time) limit. We should also mention that *p*-doped wells can exhibit a considerable intrinsic SHE (Ref. 17) since the SO interaction for heavy holes is cubic in the carrier momentum. For instance, the electrical detection of the intrinsic SHE in HgTe quantum wells via nonlocal resistance measurements shows an enhanced signal as the gate voltage controlling the carrier density is tuned from *n*-type to *p*-type conduction (Ref. 38).

[22] M. Koenig, H. Buhmann, L. W. Molenkamp, T. L. Hughes, C.-X. Liu, X.-L. Qi, and S.-C. Zhang, arXiv:0801.0901, special issue of J. Phys. Soc. Jpn. (to be published); S. Takahashi and S. Maekawa, Sci. Technol. Adv. Mater. **9**, 014105 (2008).

[23] E. Bernardes, J. Schliemann, M. Lee, J. C. Egues, and D. Loss, Phys. Rev. Lett. **99**, 076603 (2007).

[24] R. S. Calsaverini, E. Bernardes, J. C. Egues, and D. Loss, Phys. Rev. B **78**, 155313 (2008).

[25] This is "the quantum of spin conductance," the analog to the quantum of charge conductance $g = e^2/h$; these are related by $\sigma_0 = (\hbar/2e)g = e/4\pi$.

[26] For the $B=0$ the energy spectrum is $\mathcal{E}_{k_\parallel \lambda \sigma} = \hbar^2 k_\parallel^2/2m + \overline{\mathcal{E}} + \lambda \sqrt{(\Delta \mathcal{E}/2)^2 + \eta^2 k_\parallel^2}$, where $k_\parallel$ is the in-plane electron wave vector, $\lambda = \pm$ is the subband index, and $\sigma = \uparrow, \downarrow$ is the spin index. To obtain the expression, Eq. (16) for $\mathcal{E}_F$, we assume that $\eta k_\parallel \ll \Delta \mathcal{E}$ (this is a good approximation for the areal densities used).

[27] All other relevant band parameters can be found in Table III of Ref. 24 (see also Ref. 39 for further information on the band-structure parameters).

[28] Similarly to Ref. 24, here we perform the self-consistent calculation to determine the intersubband SO couplint η by considering a quantum well with a constant chemical potential (see Refs.

40 and 41 for wells with constant chemical potentials); as in Ref. 24, similar results can be obtained for the case of a constant density. The areal density n_{2D} of the well is varied via an additional gate which shifts the bottom of the potential well with respect to the fixed chemical potential level.

[29] H. Mirhosseini, J. Henk, A. Ernst, S. Ostanin, C.-T. Chiang, P. Yu, A. Winkelmann, and J. Kirschner, Phys. Rev. B **79**, 245428 (2009).

[30] N. Sugimoto, S. Onoda, S. Murakami, and N. Nagaosa, Phys. Rev. B **73**, 113305 (2006).

[31] P. G. Silvestrov, V. A. Zyuzin, and E. G. Mishchenko, Phys. Rev. Lett. **102**, 196802 (2009).

[32] S. I. Erlingsson, J. Carlos Egues, and Daniel Loss, Physica E (Amsterdam) **40**, 1484 (2008).

[33] B. K. Nikolić, S. Souma, L. P. Zârbo, and J. Sinova, Phys. Rev. Lett. **95**, 046601 (2005); B. K. Nikolić, L. P. Zârbo, and S. Souma, Phys. Rev. B **72**, 075361 (2005); S. Souma and B. K. Nikolić, Phys. Rev. Lett. **94**, 106602 (2005); G. Usaj and C. Balseiro, Europhys. Lett. **72**, 631 (2005).

[34] M. Lee and M.-S. Choi, Phys. Rev. B **71**, 153306 (2005).

[35] A. Reynoso, G. Usaj, and C. A. Balseiro, Phys. Rev. B **73**, 115342 (2006).

[36] J. Yao and Z. Q. Yang, Phys. Rev. B **73**, 033314 (2006).

[37] M. Duckheim and D. Loss, Nat. Phys. **2**, 195 (2006).

[38] C. Brüne, A. Roth, E. G. Novik, M. Koenig, H. Buhmann, E. M. Hankiewicz, W. Hanke, J. Sinova, and L. W. Molenkamp, arXiv:0812.3768 (unpublished).

[39] I. Vurgaftman, J. R. Meyer, and L. R. Ram-Mohan, J. Appl. Phys. **89**, 5815 (2001).

[40] T. Koga, J. Nitta, T. Akazaki, and H. Takayanagi, Phys. Rev. Lett. **89**, 046801 (2002).

[41] T. Koga, Y. Sekine, and J. Nitta, Phys. Rev. B **74**, 041302(R) (2006).